Chemistry and Materials Research, Vol.5 2013
Special Issue for International Congress on Materials & Structural Stability, Rabat, Morocco, 27-30 November 2013

Moisture transport in concrete during wetting/drying cycles

A. Taher[1], X. Cao[2], I.S. Pop[2], A.J.J van der Zanden[1] and H.J.H Brouwers[1]
[1] Eindhoven University of Technology, Department of the Built Environment, Eindhoven, the Netherlands
[2] Eindhoven University of Technology, Department of Mathematics and Computer Science, Eindhoven, The Netherlands

Abstact. An accurate description of moisture transport in concrete is significant to determine the service life of a concrete structure. Many authors managed to describe the global moisture transport in concrete during wetting/drying cycles by using Fick's laws of diffusion. The difference between the models of the various authors lies in the use of the diffusion coefficient. There are authors who are convinced that by using two different diffusion coefficients, one for wetting and the other for drying, a better description of the moisture transport in concrete can be obtained. In this paper, this approach is examined by simulating and comparing two models, one with a single diffusion coefficient and the other with two diffusion coefficients. A comparison is made between the results of a model with two diffusion coefficients and a model with a single diffusion coefficient, where the diffusion coefficient is the average of the wetting and drying diffusion coefficient. The result is computed for one cycle of wetting and drying. The simulations show that there are differences in the results of the models. In order to validate the model and to investigate which of the models describes the moisture transport most accurately, experimental work is needed.

1 Introduction

The durability of concrete is related to the description of moisture transport. Moisture transport in marine environment, where drying and wetting cycles occur, leads chloride to penetrate into reinforced concrete structures. When chloride reaches the rebars, corrosion can appear and that decreases the service life time of the structures. By describing the moisture transport in such a structure, the service life can be determined. Many descriptions of moisture transport in concrete can be found in the literature. For example, the authors [1-5] describe moisture transport in concrete structures by using a single diffusion coefficient. In [6-8], the same by using two different diffusion coefficients for drying and wetting. The purpose of this paper is to compare these two methods of describing moisture transport in concrete structures during drying/wetting cycles. In addition to the modeling, an experimental set-up is proposed to validate the models.

2 Mathematical model

In this paper, the moisture transport (one phase flow) in concrete is described based on the Darcy's law and mass balance [9]:

$$v = -\frac{\bar{k}}{\mu} k_r \nabla p_c \qquad \text{(Darcy)}, \tag{1}$$

where v is the volumetric velocity (m/s), $\bar{k}$ the intrinsic permeability of the concrete (m^2), k_r the relative permeability (-), μ the viscosity ($kg \cdot m^{-1} \cdot s^{-1}$), and p_c the capillary pressure ($kg \cdot m^{-1} \cdot s^{-2}$).

$$\frac{\partial}{\partial t}(\phi s) + \nabla \cdot v = 0 \qquad \text{(mass balance)}, \tag{2}$$

where ϕ is the porosity of the concrete (-), s the water saturation (-), and t the time (s).

Commonly, k_r and p_c are increasing functions of the saturation s, see [9].

By substituting eq.(1) into eq.(2),

$$\frac{\partial}{\partial t}(\phi s) - \nabla \cdot (\frac{\bar{k}}{\mu} k_r \nabla p_c) = 0. \tag{3}$$

Furthermore, the following is assumed in this paper:

- The sample is homogeneous.
- There is no flow at the boundaries except the boundary at the right.
- The initial saturation is constant.

(1)

For the boundary at the right, a periodic repetition of

wetting and drying cycles is assumed. In view of these assumptions, the lateral flow is 0. This allows reducing the model to one dimension. The sample occupies then the interval $(0, L)$.

The following conditions are imposed,

$$at \quad t = 0: \quad s = s_i, \qquad \text{in } (0, L), \tag{4}$$

$$at \quad x = 0: \quad \frac{\bar{k}}{\mu} k_r \frac{\partial p_c}{\partial x} = 0, \qquad t > 0, \tag{5}$$

$$at \quad x = L: \quad s = s_b(t), \qquad t > 0, \tag{6}$$

where s_i is the initial saturation, $s_b(t)$ the saturation at the right boundary.

In the context of a one-dimensional model, eq.(3) becomes

$$\frac{\partial}{\partial t}(\phi s) - \frac{\partial}{\partial x}\left(\frac{\bar{k}}{\mu} k_r \frac{\partial p_c}{\partial x}\right) = 0. \tag{7}$$

To make the equation dimensionless, the following notations are introduced,

$$x := \frac{x}{L}, \quad t := \frac{t}{T}, \quad p_c := \frac{p_c}{P}, \tag{8}$$

where L, T, P are characteristic values for the length, time, and capillary pressure. Substitute eq.(8) into eq.(7) and set,

$$\frac{T}{L^2} = \frac{\phi \mu}{\bar{k} P}, \tag{9}$$

then eq.(7) transforms into,

$$\frac{\partial s}{\partial t} = \frac{\partial}{\partial x}\left(D(s)\frac{\partial s}{\partial x}\right). \tag{10}$$

Here

$$D(s) = k_r(s) \cdot \frac{dp_c(s)}{ds}. \tag{11}$$

By using the Kirchhoff transformation

$$\beta(s) = \int_0^s D(v)dv, \tag{12}$$

eq.(10) becomes

$$\frac{\partial s}{\partial t} = \Delta\beta(s), \tag{13}$$

while the initial and boundary conditions are,

$$s(x,0) = s_i, \quad \frac{\partial s}{\partial x}(0,t) = 0, \quad s(1,t) = s_b(t), \tag{14}$$

where s_i is a constant number between 0 (in case of dried concrete) and 1 (in case of water saturated concrete). $s_b(t)$ is a periodic function, which simulates wetting/drying cycles,

$$s_b(t) = \begin{cases} 1 & t \in (0, T_w] + k \cdot T_p, \\ 0 & t \in (T_w, T_p] + k \cdot T_p, \end{cases} \tag{15}$$

where T_d is the dimensionless drying time, T_w is the dimensionless wetting time, $T_p = T_d + T_w$, is the period of one cycle, and k is any natural numbers.

3 Approaches

Two modeling approaches for the moisture transport in concrete are compared in this paper. The first model uses the same diffusion coefficient for both wetting and drying phase. The second model uses two diffusion coefficients, one for the drying $D^-(s)$ and one for the wetting $D^+(s)$.

In the literature [8], these following coefficients are determined experimentally ,

$$D^+(s) = 10^{-10} \cdot e^{6 \cdot s}, \tag{16}$$

$$D^-(s) = 10^{-10} \cdot \left(0.025 + \frac{0.975}{1 + \left(\frac{1-s}{0.208}\right)^6}\right), \tag{17}$$

which are plotted in Figure 1.

3.1 Standard model: one diffusion coefficient

A standard model considers the same diffusion coefficient for both wetting and drying, In view of eq.(16) and eq.(17), the following averages are considered,

$$D_a(s) = \frac{D^+(s) + D^-(s)}{2}, \tag{18}$$

$$D_g(s) = \sqrt{D^+(s) \cdot D^-(s)}. \tag{19}$$

Here $D_a(s)$ is the arithmetic average of the diffusion coefficients, $D_g(s)$ the logarithmical average of the diffusion coefficients, $D^+(s)$ the diffusion coefficient for wetting and $D^-(s)$ the diffusion coefficient for drying.

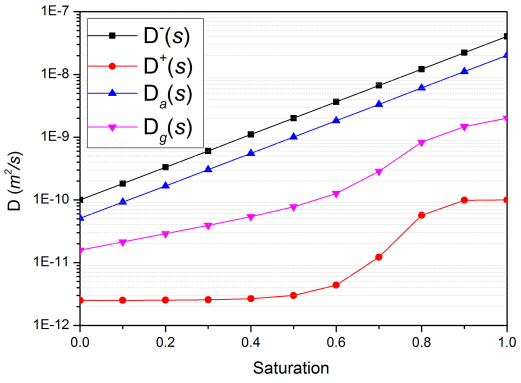

Fig. 1. Various diffusion coefficients as a function of saturation

The coefficients introduced in eq.(18) and (19) are then used for the Kirchhoff transformation in eq.(10). For the resulting model, eq.(12), an implicit numerical scheme [10] is combined with a linear iterative procedure [11].

3.2 Hysteretic model

Here the hysteretic model in [12] is adapted,

$$\frac{\partial s}{\partial t} = \partial_{xx} p(s). \tag{20}$$

In the above, $p(s)$ has to include the switch between two diffusion coefficients, in this case, $p(s)$ reads,

$$p(s) = p_e(s) + \gamma(s) sign(\partial_t s), \tag{21}$$

where $p_e(s)$, $\gamma(s)$ and $sign(\partial_t s)$ are defined as

$$p_e(s) = \frac{\beta^+(s) + \beta^-(s)}{2}, \tag{22}$$

$$\gamma(s) = \frac{\beta^+(s) - \beta^-(s)}{2}, \tag{23}$$

and

$$sign(\partial_t s) = \begin{cases} 1 & if \quad \partial_t s > 0, \\ -1 & if \quad \partial_t s < 0. \end{cases} \tag{24}$$

$\beta^{+/-}(s)$ are the Kirchhoff transformations for the wetting/drying diffusion coefficients ,

$$\beta^{+/-}(s) = \int_0^s D(z)^{+/-} dz. \tag{25}$$

When solving the system, $sign(\partial_t s)$ is replaced by the regularization $sign_\delta(\partial_t s)$ (see Figure 2),

$$sign_\delta(\partial_t s) = \begin{cases} \delta \partial_t s + \delta^2 - 1 & if \quad \partial_t s < \delta, \\ \dfrac{\partial_t s}{\delta} & if \quad -\delta < \partial_t s < \delta, \\ \delta \partial_t s - \delta^2 + 1 & if \quad \partial_t s > \delta, \end{cases} \tag{26}$$

where $0 < \delta << 1$ is the regularization parameter.

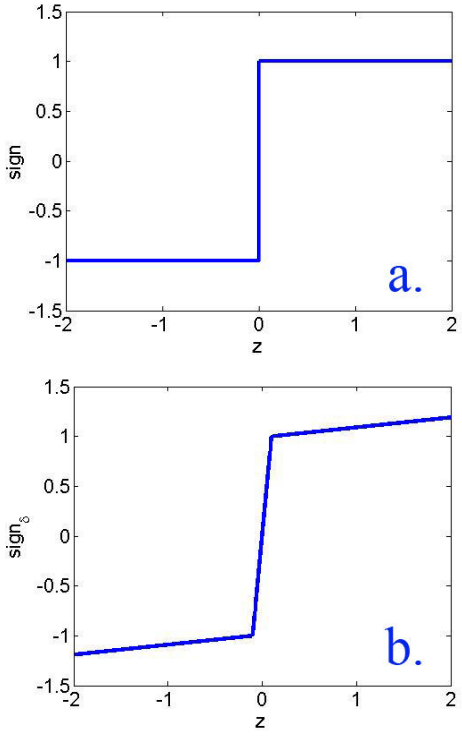

Fig. 2. The graphs of (a.) $sign$ and (b.) $sign_\delta$

Solving the above equations directly using finite difference method leads to incorrect results. Alternatively, the inverse $\phi_\delta(r)$ of the regularized $sign_\delta$ is used as considered in [13],

$$\phi_\delta(r) := \begin{cases} -\delta + \dfrac{r+1}{\delta} & if \quad r < -\delta, \\ \delta r & if \quad r \in [-\delta, \delta], \\ \delta + \dfrac{r-1}{\delta} & if \quad r > \delta, \end{cases} \tag{27}$$

For the time discretization, let Δt be the time step, and $p^m \approx p(m \cdot \Delta t)$, $s^m \approx s(m \cdot \Delta t)$

The implicit discretization of eq.(20)and eq.(21) are:

$$\frac{s^{m+1}-s^m}{\Delta t} = \partial_{xx} p^{m+1},$$
$$\frac{s^{m+1}-s^m}{\Delta t} = \phi_\delta\left(\frac{p^{m+1}-p_e(s^{m+1})}{\gamma(s^m)}\right), \quad (28)$$

where $m = 0,1,\ldots$ initially, $s^0 = s_i$.

Further, at $x = 0$, $\partial_x p^{m+1} = 0$, and

at $x = L$, $s^{m+1} = s_b((m+1)\Delta t)$.

In the equations above, eq.(28) and the left side of eq.(29) are explicit for s^{m+1}. The right side of eq.(29) is implicit for s^{m+1}, due to the nonlinear function of $p_e(s)$. Therefore, $p_e(s^{m+1})$ is simplified for a linear function as investigated in [14] by a Taylor expansion given by

$$p_e(s^{m+1}) = p_e(s^m) + p_e'(s^m)\cdot(s^{m+1}-s^m). \quad (29)$$

Then the discretized form becomes

$$\frac{s^{m+1}-s^m}{\Delta t} = \partial_{xx} p^{m+1},$$
$$\frac{s^{m+1}-s^m}{\Delta t} = \phi_\delta\left(\frac{p^{m+1}-p_e(s^m)-p_e'(s^m)\cdot(s^{m+1}-s^m)}{\gamma(s^m)}\right). \quad (30)$$

For discretizing the spatial derivatives, finite differences on a grid with $\Delta x = 1/N$ $(N \in \mathrm{N})$ are used.

4 Numerical results

The model is implemented in Matlab. Here, only one cycle is computed, which is one day for wetting and six days for drying. The initial condition (c_i) in this case is assumed to be 50% saturation. Further, the following is used in the numerical scheme: $\delta = 10^{-5}$, and $\Delta x = 10^{-3}, dt = 10^{-6}$.

The comparison between the results of the standard model with one diffusion coefficient and the results of the hysteretic model with two diffusion coefficients are shown in Figure 3.

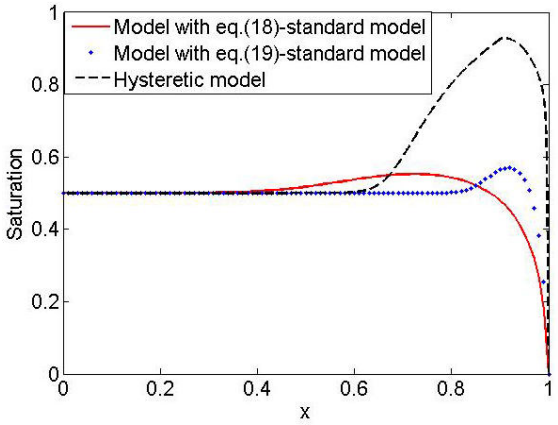

Fig. 3. Comparison of the models

The results show that there is a large difference between the three models. To validate the models, experimental work is needed, which will be explained in the next section.

5 Experiment

Mortar specimens with a water cement ratio of 0.5 and cement type of CEM I 42.5 N are used in this paper to validate the models. Mortar specimens are prepared by casting them in PVC tubes with a diameter of 100 mm. After one day, the mortar is demoulded and cured for 28 days. The side of the specimens is sealed with epoxy to ensure a one dimensional flux. At one of the two open surfaces of the specimen, the condition is changed to simulate cycles. Wetting is simulated by contacting the surface with water during one day and drying by blowing dry air with a certain flow at the surface during 6 days. After one drying/wetting cycle (one week), the moisture content is determined by weighing the specimen. This mass is compared with the calculated mass from the moisture profiles of the models for validation. Figure 4, shows the experimental setup.

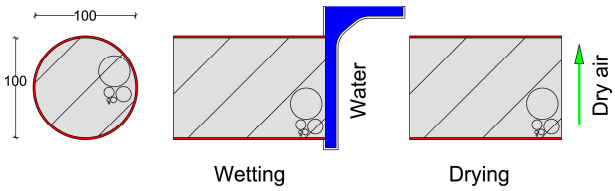

Fig. 4. Sealed mortar specimens encounter wetting cycle for one day and drying cycle for six days

6 Conclusions

Two various methods (standard method and hysteretic method) to describe moisture transport in concrete during wetting/drying cycles are implemented in Matlab and the results are compared. Measured diffusion coefficient in the

literature is used in the models. One cycle of wetting/drying is compared. The duration of the wetting phase is one day and drying is six days. From the obtained numerical results, it can be concluded, that using the standard model with one diffusion coefficient or using the hysteretic model with two diffusion coefficients, can have a large influence on the results. After one cycle, the hysteretic model gives clearly a higher amount of moisture content in the structure, as it is shown in Figure 3. Furthermore, an experiment set-up is designed to validate the models.

References

1. S.J.H. Meijers, J.M.J.M. Bijen, R. de Borst, A.L.A. Fraaij, Computational results of a model for chloride ingress in concrete including convection, drying-wetting cycles and carbonation. Materials and structures; **38** pp. 145-154 (2005).
2. J. Arfvidsson, A new algorithm to calculate the isothermal moisture penetration for periodically varying relative humidity at the boundary. Nordic Journal of Building Physics; **2** (1999).
3. M.J. Cunningham, Moisture diffusion due to periodic moisture and temperature boundary conditions Çöan approximate steady analytical solution with non-constant diffusion coefficients. Building and Environment; **27** pp. 367-377 (1992).
4. L. Pel, *Moisture transport in porous building materials* (1995).
5. A. Selander, *Hydrophobic Impregnation of Concrete Structures: Effects on Concrete Properties* (2010).
6. J.M. Torrenti, L. Granger, M. Diruy, P. Genin, Modeling concrete shrinkage under variable ambient conditions. ACI Materials Journal; **96** (1999).
7. V. Baroghel-Bouny, Caractérisation des pâtes de ciment et des bétons-Méthodes, analyse, interprétations (1994).
8. C. Li, K. Li, Z. Chen, Numerical analysis of moisture influential depth in conrete during drying-wetting cycles. Tsinghua Science & Technology; **13**, pp. 696–701 (2008).
9. F. G. Pinder, G. W. Gray, *Essentials of Multiphase Flow and Transport in Porous Media*, John Wiley & Sons, Inc. (2008).
10. F.A. Radu, I.S. Pop, P. Knabner, Error estimates for a mixed finite element discretization of some degenerate parabolic equations, Numerische Mathematik; **109**, pp. 285-311 (2008).
11. F.A. Radu, I.S. Pop, P. Knabner, Newton type methods for the mixed finite element discretization of some degenerate parabolic equations, in *Numerical Mathematics and Advanced Applications*, A. Bermudez de Castro, D. Gomez, P. Quintela, P. Salgado (Eds.), Springer-Verlag Heidelberg; pp. 1192 – 1200 (2006).
12. A. Yu. Beliaev, S. M. Hassanizaeh, A theoretical model of hysteresis and dynamic effects in the capillary relation for two-phase flow in porous media. Transport in Porous Media; **43** pp 487–510 (2001).
13. B. Schweizer, Instability of gravity wetting fronts for Richards equations with hysteresis, Interfaces and Free Boundaries; **14**, pp. 37-64 (2012).
14. A. Rätz, B. Schweizer, Hysteresis models and gravity fingering in porous media, ZAMM - Journal of Applied Mathematics and Mechanics. (2012).